2016

Analysis of Vibration Isolators for Hermetic Compressors

Carlos Eduardo Vendrami
Embraco, Brazil, carlos.vendrami@embraco.com

Claudio Pellegrini
Embraco, Brazil, claudio.pellegrini@embraco.com

Analysis of Vibration Isolators for Hermetic Compressors

Carlos Eduardo VENDRAMI*, Claudio PELLEGRINI

Embraco, Research & Development
Joinville, SC, Brazil
Phone: +55 47 3441-2650, carlos_vendrami@embraco.com.br

* Corresponding Author

ABSTRACT

Recently, the customers of refrigerators and freezers have become more exigent in respect to the acoustic comfort of these home appliances. Among the noise sources, there are the refrigerant flow, the fans and the compressors. The compressors might be responsible for a part of the cabinet low frequency noise, which could be generated either by the gas pulsation that excites the tubing or the compressor low frequency vibration that transfers energy to the cabinet base plate and tubing.

The compressor low frequency vibration is a function of the mechanism loads and the gas pressure that acts on the piston and it is modulated by its running frequency and harmonics. Besides, at low frequencies, the compressor behaves as a rigid body assembled on isolators or grommets, which link the compressor to the cabinet base plate. If one knows these rigid body natural frequencies, it is possible to optimize the refrigerator project, providing a better acoustic performance for manufacturers and final customers.

Based on this context, this paper aims to present a study of the compressor grommets, usually made of rubber. First of all, an investigation about the materials is carried out using a technique with a single degree-of-freedom system. Secondly, an analysis of the static behavior of an isolator using the rubber properties is performed. Finally, a numerical model to predict the modal behavior of a compressor assembled on a rigid base is created and experimentally validated.

1. INTRODUCTION

The low frequency noise radiated by a cabinet can have some sources, such the gas flow, the fans and the compressor. Among the sources related to the compressor itself, there are the gas pulsation and the compressor low frequency vibration, which are created by mechanism loads and the gas pressure that acts on the piston.

At low frequencies the compressor behaves as a rigid body, because it is assembled on isolators or grommets which are components, normally made of rubber, that link the compressor base plate to the appliance base plate. Figure 1 presents an example of grommet assembled in a compressor and an example of grommet.

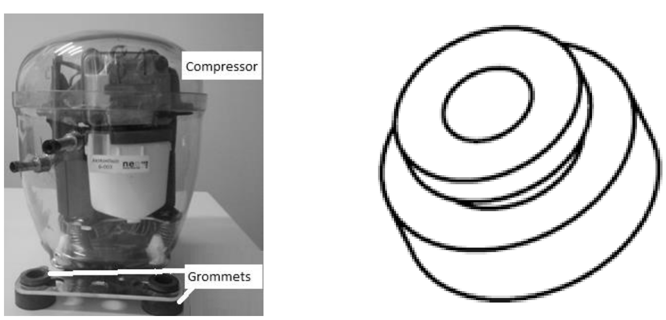

Figure 1: Compressor assembled on grommets and an example of grommet. Source: Vendrami, 2013.

Therefore, grommets are components that transfer some energy from the compressor to the appliance and because of this they can generate noise problems in low frequency. These problems are more frequent when a rigid body natural frequency of the compressor assembled on the base plate coincides with the compressor running frequency or any other critical frequency. Figure 2 shows how it is possible to optimize the low frequency noise with a good choice of grommets for a specific appliance.

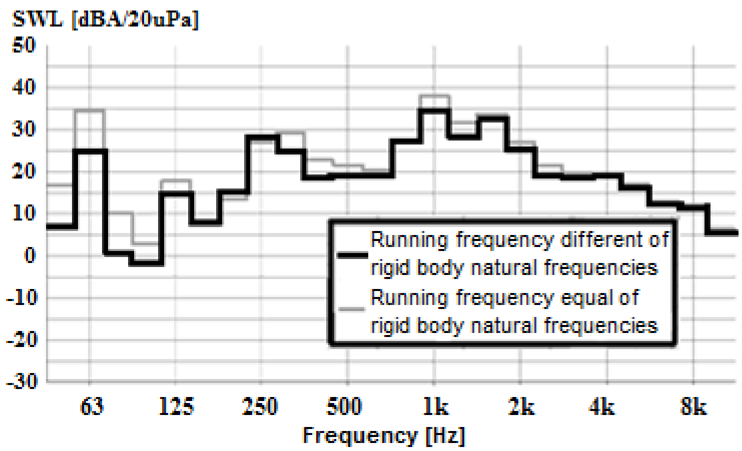

Figure 2: Low frequency noise optimization with a good choice of grommets. Source: Porto, 2010.

Knowing that nowadays customers are more and more exigent about the noise radiated by their home appliances, this work aims to present a study about the grommets, presenting some basic properties of the rubber and some ways to find out other properties. Besides, it presents some numerical static and dynamic analysis of these components as well as some validation of these simulations.

2. THE RUBBER AND ITS PROPERTIES

Rubbers are materials which have low plastic deformation, low Young Modulus (E) and are able to support deformations up to 1,000%. Besides, they have high resilience, high internal damping and do not follow the Hooke's law under deformation.

According to Istvan (2006), rubber behavior varies with the temperature. At low temperatures, the molecules are almost static and there is small relative movement between them, which means that rubbers have high Young Modulus (E), close to 0.5 (0.499 according to Jones, 2001) and small damping factor (η), respectively.

At high temperatures, the relative velocity between the molecules is higher, which means the Young Modulus tends to be smaller. As the interaction between molecules is lower, thus the loss factor is also lower.

Finally, at mid temperatures, there is small Young modulus but the loss factor is high.

Figure 3 shows the dependency of the Young Modulus and the Loss factor with the temperature for viscoelastic materials, like rubber.

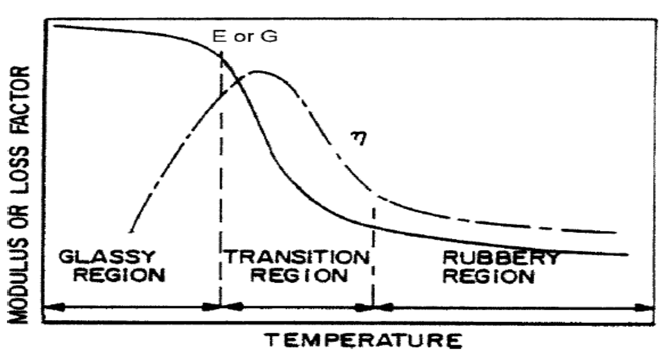

Figure 3: Variation of the Young Modulus and the Loss Factor with the temperature. Source: Istvan, Beranek, 2006.

The effect of the frequency is the opposite of the effect of the temperature: bigger the frequency of a harmonic excitation that acts on the rubber, the higher the Young Modulus (Jones, 2001).

Another property largely used to characterize a sample of rubber is the hardness, that is the resistance to the plastic deformation when an external load is applied (Almeida, 2009). Some authors created calculations and graphs which allows the association of the hardness of the rubber to its Young Modulus. One of them was proposed by Gent (1958) and correlates the Young Modulus *E*, in MPa, to Shore A hardness (*S*):

$$E = \frac{0.0981(56+7.62336S)}{0.137505(254-2.54S)} \qquad (1).$$

Next sections will show two techniques used to measure rubbers Young modulus and loss factor: Oberst Beam, presented in ASTM Standards (2005), and Single Degree of Freedom. It is important to mention that for both techniques, the system temperature must be controlled.
The last section will present the Reduced Frequency Nomogram that is used to present Young modulus and loss factor data, obtained for different frequencies and temperatures, in only two curves.

2.1 Oberst Beam Technique

According to this technique, first the frequency response of the base beam is measured using the measurement system exemplified in Figure 4A, at specific temperatures which are controlled when the apparatus is placed in an environmental chamber (Figure 4B). The Oberst beam, which is composed by the base beam and a layer of viscoelastic material, is presented in Figure 4C.

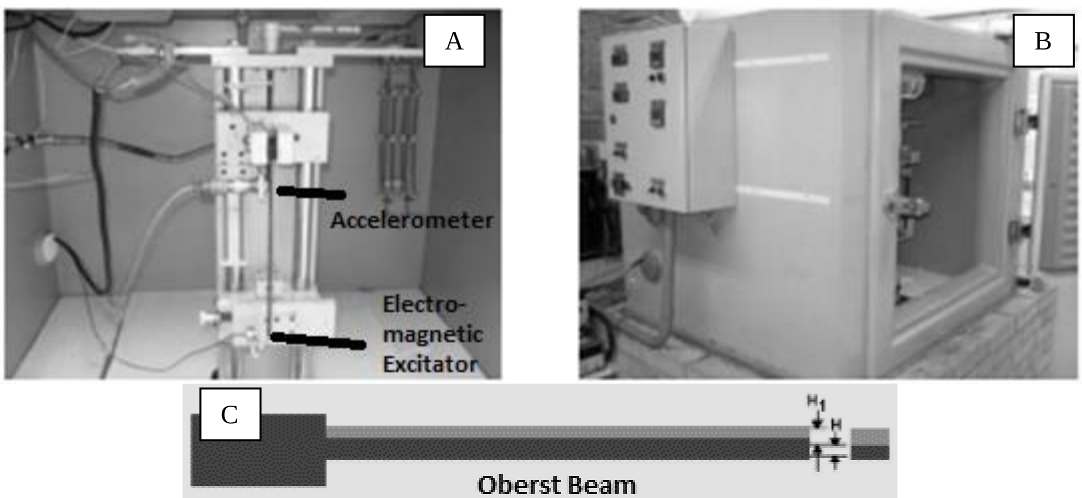

Figure 4: Apparatus to measure the frequency response (A), Environmental chamber (B) and Oberst Beam (C). Source: Stumpf, 2013.

According to ASTM Standards (2005), Young Modulus E_b and loss factor ηb of base beam material are calculated:

$$E_b = \frac{12\rho_b.L^4 {f_n}^2}{H^2 {C_n}^2} \qquad (2),$$

$$\eta_b = \frac{\Delta f_n}{f_n} \qquad (3).$$

where C_1 =0,55959, C_2 =3,5069, C_3 =9,8194 and $C_n = (\pi/2)(n - 0{,}5)$ for n>3, f_n are the resonance frequencies of n modes, Δf_n is the half power band ($\Delta f_n = \frac{f_{2n}-f_{1n}}{2f_n}$, where f_{2n} and f_{1n} are the two frequencies closer to f_n which the energy is the half part of the energy of the peak given for f_n, considering $f_{1n} < f_n < f_{2n}$), ρ_b is the material density, H is the thickness and L is the length.
After measuring the frequency response of the base beam, the damped beam response is also measured. This damped beam is basically composed by the base beam and a layer of rubber which is glued on the metal and its natural frequencies, the rubber Young Modulus E_v and the rubber loss factors η_v must be obtained at the same temperatures the base beam was tested, according to equations (4) and (5).

$$E_v = \frac{E_b}{(2R^3)}\left[(\alpha-\beta)+\sqrt{\{(\alpha-\beta)^2-4R^2(1-\alpha)\}}\right] \quad (4),$$

$$\eta_v = \eta_c\left[\frac{(1+MR)(1+4MR+6MR^2+4MR^3+M^2R^4)}{(MR)(3+6R+4R^2+2MR^3+M^2R^4)}\right], \quad (5),$$

where c is an index, f_n is the resonance frequency for mode n of base beam, f_c is the resonance frequency of the mode c of the composed beam, Δf_c is the half power band of mode c of the composed beam (calculated as Δf_n), H_1 is rubber layer thickness, $M = \frac{E_v}{E_b}$, $R = \frac{H_1}{H}$, $\alpha = (f_c/f_n)^2\left(1+\frac{\rho_v}{\rho_b}R\right)$, $\beta = 4+6R+4R^2$, $\eta_c = \Delta f_c/f_c$ is the composed beam loss factor and ρ_v is rubber density. This technique is indicated specially for determining properties of materials with Young modulus over than 100MPa (ASTM Standards, 2005), value normally higher than rubbers commonly used in grommets.

2.2 Single Degree of Freedom Technique

Another technique that might be used for the analysis of the rubber properties is the single degree of freedom technique. In this case, the dynamic properties are evaluated in tests which a cylindrical rubber sample is glued on a flat surface that needs to be sufficiently stiff. On the rubber sample upper surface, it is necessary to glue a steel cylindrical block (rubber sample and steel block must have the same central axis) with a mass much bigger than the rubber sample mass.

Then, this system is then placed inside an environmental chamber like the one showed in Figure 4B at a specific temperature and must be excited with a sweep sine signal, using a shaker. In this case, the rubber sample behaves as a spring and the steel block has a point mass behavior.

The frequency response of the point mass related to the base is obtained using two accelerometers (both *B&K* type 4517) as showed in Figure 5.

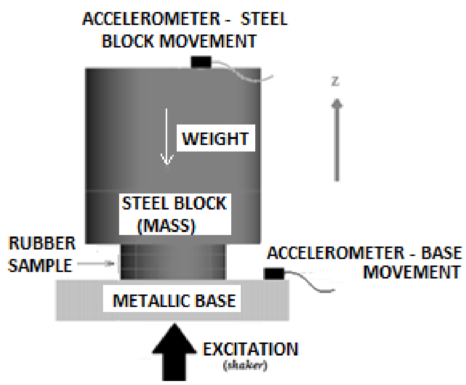

Figure 5: Measurement system for single degree of Freedom Technique. Source: Vendrami, 2013.

Considering the same rubber sample and three different steel blocks with masses A, B and C and using the measurement system presented in Figure 5, curves like the ones presented in Figure 6 are obtained.

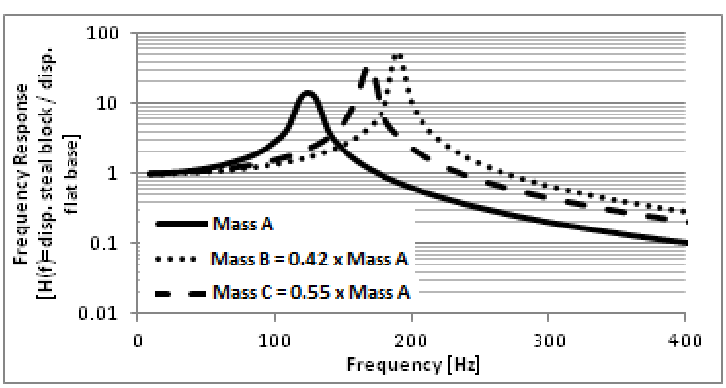

Figure 6: Example of experimental curves obtained with Single Degree of Freedom Technique.

The rubber loss factor normally is obtained directly from the curves at the peaks. For example, *B&K Pulse 12.0* uses half Power band to calculate the damping factor ζ, which is the half part of the loss factor.
On the other hand, the rubber Young modulus needs to be obtained adjusting a numerical model to the experiment. For this purpose, it is necessary to set in the numerical model the density and the Poisson's ratio of the rubber sample material as well as the density, the Poisson's ratio and the Young modulus of the steel.
Using all these properties, some numerical modal analysis can be done, varying in the software the value of rubber Young modulus until the system first natural frequency results similar (difference between the experiment and the simulation lower than 0.1%) to the frequency of the peak obtained during the experiments. To do this numerical modal analysis, one must consider fixed all the nodes of rubber lower surface and common nodes at the interface between the rubber sample and the steel block.
This technique is interesting to calculate the dynamic properties of the rubbers commonly used in grommets, which the Young Modulus for frequencies up to 400Hz is lower than 50 MPa.

2.3 Reduced Frequency Nomogram

As already commented, the Reduced Frequency Nomogram is a way to present Young Modulus and Loss Factor magnitudes, obtained at different temperatures and frequencies, using only two curves. This fact allows extrapolation of these parameters to frequency and temperature ranges that were not evaluated (ASTM Standards, 2005).
This Nomogram is obtained from the Superposition Principle that affirms the dynamic properties as E and η of the rubber are function of the product $f \times \alpha_T(T)$ where *f* is the frequency and α_T is the shift factor, that is a function of the temperature *T*. The product $f \times \alpha_T(T) = f_R$, where f_R is also known as reduced frequency.
Based on these concepts, the Young Modulus and the Loss Factor can be defined as follows:

$$E = E(f,T) = E\big(f.\alpha_T(T)\big) = E(f_R) \qquad (6),$$

$$\eta = \eta(f,T) = \eta\big(f.\alpha_T(T)\big) = \eta(f_R) \qquad (7).$$

Finally, for Reduced Frequency Nomograms consolidation, it is necessary to calculate the shift factor $\alpha_T(T)$. Williams, Landel and Ferry (1955) proposed an WLF equation to do this calculation:

$$log[\alpha_T(T)] = -C_1 \frac{T-T_0}{B_1+T-T_0} \qquad (8),$$

where B_1 and C_1 are constants which must be determined. Osswald (2010) suggests some values for these constants, and *T0* is the temperature where there is the transition from glassy region to transition region of the material.
Based on the loss factors measured and Young Modulus and Reduced frequencies calculated at different temperatures, it is possible to create the nomograms as the one showed in Figure 7.

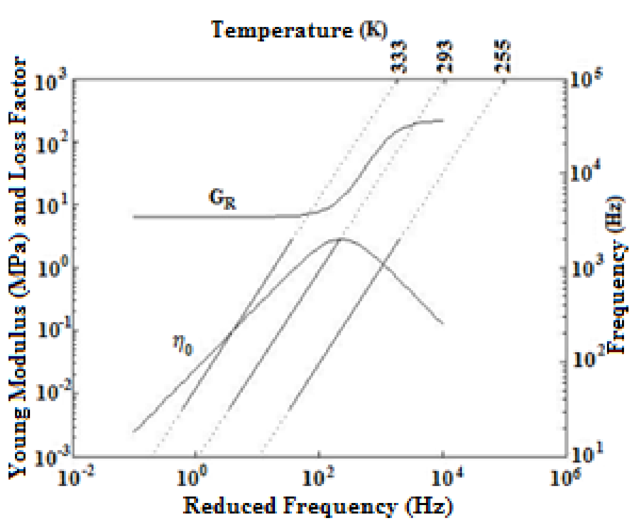

Figure 7: Reduced Frequency Nomogram Example. Source: Medeiros Júnior, 2010

Further recommendation to create and to use Reduced Frequency Nomograms, which are necessary to correctly set rubber dynamic properties for grommet analysis and projects, are found in ASTM Standards (2005).

3. GROMMET STATIC ANALYSIS

The first analysis done to understand the characteristics of a grommet was a static analysis. This analysis is important to understand how much the grommet structure deforms because of compressor weight.

3.1 Numerical Model

A FEM numerical model can be defined to understand grommet behavior under the compressor's weight load.
To set the properties to do this type of analysis, the construction of Reduced Frequency Nomograms is not necessary, but it is mandatory to consider the Poisson's ratio, the density and the rubber static Young Modulus E_0. This value can be obtained by several ways, especially from the rubber material hardness, using calculations like the one proposed by Gent (1958).
The geometric model must consider only grommet utile part for the point of view of the stiffness which is the part that is under compressor base plate as it is showed in Figure 8.

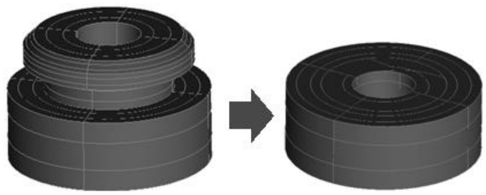

Figure 8: Schematic representation of the analyzed grommet (L) and its functional part (R). Source: Vendrami, 2013.

For the model, a hexahedrical mesh (element SOLID185) was created and using *ANSYS 11.0*, all the nodes of the grommet lower surface are considered fixed. On the upper surface, a displacement from 0.02 up to 0.5mm in intervals of 0.02mm was imposed, knowing the fact that 0.5mm is bigger than the deformation imposed by most of compressors (Porto, 2010).
The goal of the simulation is to calculate the reaction force, in newtons, at the lower surface for each increment of displacement, as the outline presented in Figure 9 proposes.

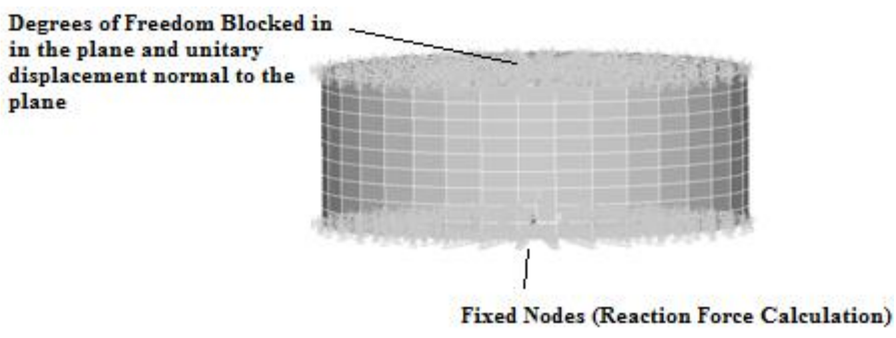

Figure 9: Schematic representation of the simulation.

The result for the proposed grommet showed a straight line in a chart Force vs. Displacement, where its inclination represents the grommet stiffness given in N/mm.

3.2 Model Validation

For the validation of the static numerical model, a Universal Testing Machine (model EMIC DL2000) was used in order to obtain a curve of the reaction force, in N, at the lower surface as a function of deformation imposed at the upper surface, in mm. The speed of the grommet deformation was set as 1mm/min.

Figure 10 presents the equipment and the position of the grommets for the described test and how the grommet sample was prepared.

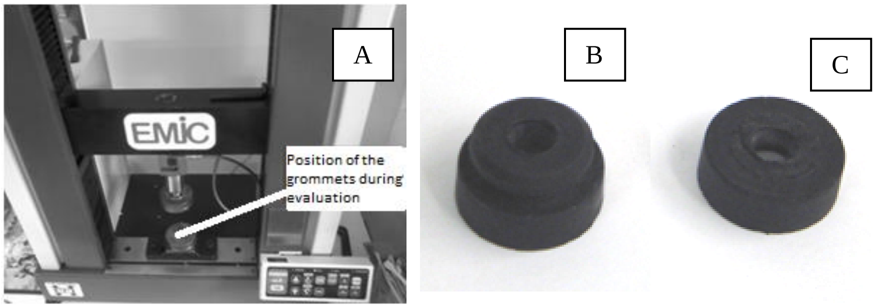

Figure 10: Equipment used for the experiments (A), entire grommet used in the analysis (B) and its utile part (C).

A comparison of the numerical and experimental curves (Figure 11) suggests a good correlation between the results due to a difference lower than 3% in the reaction force, with higher forces for the numerical curve.

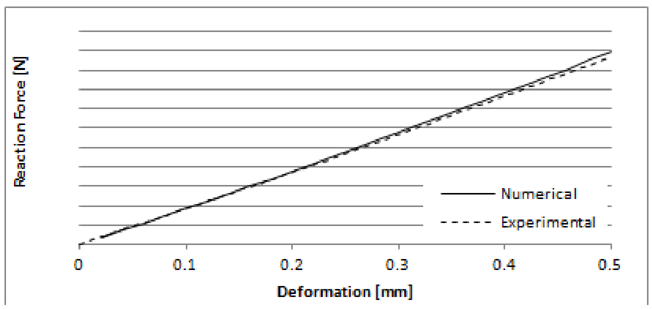

Figure 11: Numerical vs. Experimental Grommet static behavior.

4. MODAL ANALYSIS: COMPRESSOR ASSEMBLED ON GROMMETS

4.1 Simplified Model

In order to simplify the model, focusing on the grommet model (because the emphasis of this work is in frequencies up to 400Hz), the compressor geometry was simplified, representing it with steel block with total mass and *W* and *LB* dimensions similar to the ones of a typical compressor. Dimension *H* is around 20% of a typical reciprocating compressor.
Figure 12 shows the simplified model where two base plates are welded, with grommets assembled to them.

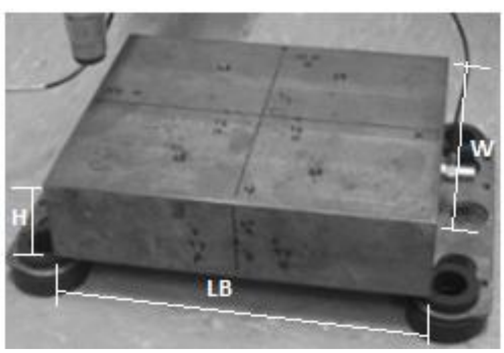

Figure 12: Steel block used to simplify the compressor geometry.

4.2 Numerical Model

For the modal analysis to determine the natural frequencies and modes of the system presented in Figure 12, a commercial software can be used. For the proposed range of frequencies, it is expected to find out six modes: in

three of them the dominant movement is a translation (in three orthogonal directions) and in three of them the dominant movement is a rotation (the three rotation axis should be orthogonal).
The first parameters that must be set are the material properties: for the block and base plates, standard steel properties are used; for the grommets, the properties defined for a static condition (commented on session 3.1) and dynamic condition (from nomograms like the one showed in Figure 7) are used.
The second step is to create the system mesh: the steel block can be modeled as a rigid body, while the base plates are modeled with quadratic tetrahedral elements and the grommets with quadratic hexahedral elements.
After finishing the mesh, the boundary conditions and joints are defined: the nodes of the lower grommet surfaces are fixed and fixed-fixed joints are created between the grommets and the base plates as well as between the base plates and the steel block.
The first analysis is a static analysis (static properties for the grommet), used to calculate the grommet deformation due to the gravity acceleration which is considered 9.8m/s^2.
Considering the deformed mesh obtained from the static analysis, a modal analysis with *Block Lanczos* algorithm is launch. The following steps were followed:

a) The first 6 natural frequencies are calculated for Young modulus E_{Mat} at 10Hz and 25ºC in order to have a first approach for all of the rigid body frequencies.
b) For each of the six natural frequencies, Young Modulus E_{Mat} is recalculated, using the equation that defines it at 25ºC. This equation is based on the rubber Reduced Frequency Nomogram and is defined as it follows:

$$E_{Mat}(f) = C1\ln(f) + C2 \qquad (9),$$

where $C1$ and $C2$ are constants obtained from the nomogram and f is each one of the natural frequencies obtained from the software. The modal analysis must be redone for all the six natural frequencies, varying the dynamic Young Modulus, up to the value of E_{Mat} at equation (9) is equal to the value of dynamic Young Modulus set.

The results for the dimensionless natural frequencies are in Table 1 and two mode shapes are presented in Figure 13. The dimensionless natural frequency ${f^*}_n$ of mode *n* is defined by equation (10):

$${f^*}_n = {f_n}/{f_1} \qquad (10),$$

where f_n is the value of the natural frequency of mode *n* and f_1 is the natural frequency of the first mode.

Table 1: dimensionless natural frequencies of Figure 14 system.

Number of mode	***#1***	**#2**	**#3**	**#4**	**#5**	**#6**
${f^*}_n$	1.00	1.06	1.78	2.34	2.46	4.78

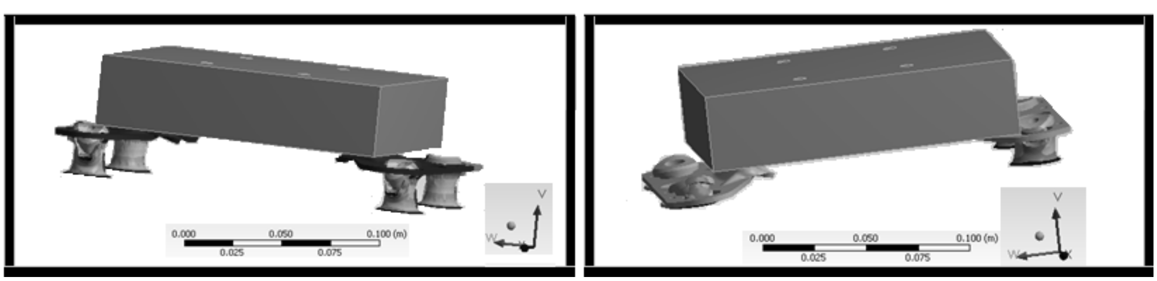

Figure 13: Mode with dominant translation movement at V axis and mode with dominant rotation movement around X direction.

4.3 Model Validation

The steel block presented in Figure 12 was used to do the validation as well as an impact hammer (*B&K* type *8202*) with rubber tip and a uniaxial accelerometer (*B&K* type 4397). Glue connected the grommets to the base plate and the grommets to the rigid base where the experiments toke place.
For the hammer force transducer, a transient window was set (the FFT must contain only the force peak generated by the hummer excitation), while for the accelerometer an exponential window was defined (the sinusoidal response

decreases with the time because of the rubber internal damping). With these settings using *B&K Pulse 12.0*, it was possible to obtain all the six rigid body natural frequencies, considering the range of interest until 400Hz.
The accelerometer and the impact position with the hammer are important to excite the rigid body modes. Figure 14 shows how to excite and measure the response of two different modes and a typical response curve.

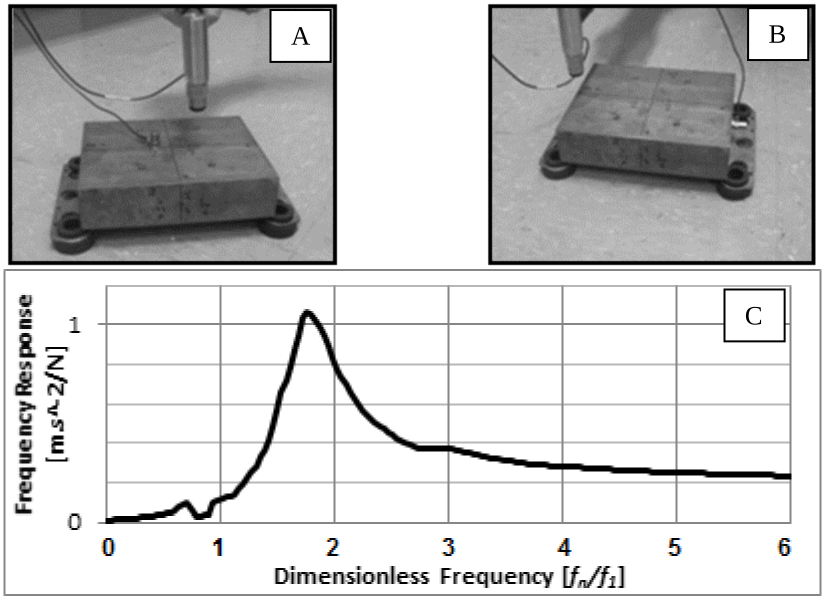

Figure 14: Excitation and measurement of a mode with dominant translation movement at V axis (A) and rotation movement around X direction (B) and typical response curve (C).

Table 2 shows a comparison between numerical and experimental results in terms of natural frequencies. The *Difference*, in %, is calculated according to equation (11), where *Num* represents the natural frequency calculated by *ANSYS* and *Exp* is the one obtained from the experiments.

$$Difference[\%] = \left(\frac{Exp - Num}{Num}\right).100\% \tag{11}$$

Table 2: Comparison between numerical and experimental dimensionless natural frequencies.

Mode	Numerical	Experimental	Difference
	f^*_n	f^*_n	%
#1	1.00	1.04	3.8
#2	1.06	1.15	8.9
#3	1.78	1.84	3.6
#4	2.34	2.23	-4.5
#5	2.46	2.54	3.2
#6	4.78	4.53	-5.2

It is observed from Table 2 that numerical and experimental results are very similar, therefore validating the numerical model.
Based on this model, it is possible to analyze, design and optimize grommets.

5. CONCLUSIONS

- This paper presented the importance of vibration isolators, also known as grommets, and how a good grommet choice or project may optimize appliance noise in the range from 0 to 400Hz third octave bands.

- The main properties of the rubber, the material which usually is used to made grommets, were presented as well as Oberst Beam and Single Degree of Freedom Techniques. It was shown Single Degree of Freedom Technique is a good approach to determine rubber dynamic properties. With this technique it is possible to create a Reduced Frequency Nomogram, a graph that shows the Young Modulus and the Loss Factor as a function of the temperature and the frequency

- It was presented a grommet static analysis and its validation; the results showed a difference of around 3% between numerical and experimental results.

- Based on the static analysis and using a modal analysis with grommet pre-deformation, a simplified model of a compressor assembled on grommets was analyzed, showing its six rigid body natural frequencies and some of its modes. This model was validated experimentally, showing differences lower than 10% between numerical and experimental results.

- Obtaining the rubber properties from the Single Degree of Freedom technique and using the static and the dynamic models presented in this paper, it is possible to analyze, design and optimize vibration isolator for refrigeration compressors.

REFERENCES

Almeida, C. M. (2009). *Caracterização de defeitos mecânicos produzidos por nanoindentação no InP*. Rio de Janeiro, Brazil: Rio de Janeiro Catholic University.

American Society for Testing and Materials International (2005). *ASTM E0756 – 05: Standard Test Method for Measuring Vibration-Damping Properties of Materials*. West Conshohocken, PA.

Gent, A. N. (1958). On the relation between indentation hardness and Young's modulus. *Rubber Chemistry and Technology, 31(4),* 896-906.

Istvan, L., Beranek, L. (2006). *Noise and Vibration Control Engineering - Principles and applications*: John Wiley & Sons.

Jones, D. I. G. (2001). *Handbook of Viscoelastic Vibration Damping*. Chichester: John Wiley & Sons.

Medeiros Júnior, W. B. (2010). *Caracterização Dinâmica Integrada de Elastômeros via Derivadas Fracionárias e Método GHM*. 2010. Curitiba, Brazil: Paraná Federal University.

Osswald, T. (2010). *Understanding Polymer Processing – Processes and Governing Equations*: Munich, Germany: Hanser Publishers.

Porto, L. L. R. (2010). *Simulação Numérica dos Esforços Dinâmicos de Baixas Frequências Transmitidos por Compressores Recíprocos*. Florianópolis, Brazil: Federal University of Santa Catarina.

Stumpf, C. (2013). *Determinação de Propriedades Mecânicas de Materiais Viscoelásticos através de Ajuste de Modelo*. Florianópolis, Brazil: Federal University of Santa Catarina.

Vendrami, C. E. (2013). *Análise de Isoladores de Vibração usados em Refrigeradores*. Florianópolis, Brazil: Federal University of Santa Catarina.

Williams, M. L., Landel, R. F., Ferry, J. D. (1955). The Temperature Dependence of Relaxation Mechanisms in Amorphous Polymers and Other Glass-forming Liquids. *J.Amer. Chem. Soc., 77 (14)*, 3701-3707.